

Trap-limited photovoltage in ultrathin metal oxide layers

Th. Dittrich, V. Duzhko,* and F. Koch

Technische Universität München, Physik Department E16, D-85747 Garching, Germany

V. Kytin

M.V. Lomonosov Moscow University, Physics Department, 119899 Moscow, Russia

J. Rappich

Hahn-Meitner-Institut, Abt. Silizium Photovoltaik, D-12489 Berlin, Germany

(Received 13 November 2001; published 4 April 2002)

Photovoltage signals were observed at ultrathin metal oxide ($\text{TiO}_2, \text{Cu}_2\text{O}, \text{ZnO}$)/ metal structures by transient and spectral photovoltage (PV) techniques. The sign, the spectral behavior and the time-dependent relaxation of the PV are determined by the nature of the traps in the metal oxide layers. At lower temperatures, the relaxation of the PV signal in TiO_2 layers is controlled by recombination due to the overlap of the wave functions of the spatially separated electrons and holes. At higher temperatures, thermal emission accelerates the recombination process. The Bohr radius of trapped holes, the tail of the exponential approximation of electronic states distribution above the valence band, the density of states at the valence band edge were obtained for TiO_2 layers by using the proposed model of trap limited PV. The concept of trap limited PV gives a general tool for the investigation of excess carrier separation in ultrathin metal oxide or semiconductor layers with trap states.

DOI: 10.1103/PhysRevB.65.155319

PACS number(s): 73.50.Pz, 73.50.Gr

I. INTRODUCTION

Nanoscaled materials are of great interest for interdisciplinary research due to their comparable size with molecular dimensions, biocompatibility (porous Si, porous TiO_2) and chemical reactivity of the expanded surface. For example, porous metal oxides are applied in photovoltaics,¹ biosensors,² and catalysis.³ Nanoscaled in one dimension ultrathin metal oxide layers are novel promising high- k dielectrics for electronics.⁴ The transport properties of nanoscaled metal oxides play in many cases an important role for applications. However, little is known about the basic transport mechanisms in nanoscaled materials, while usual for bulk semiconductors concepts can not be applied.

The low value of charge carrier mobility in metal oxides⁵ implies a mean free path in the order of the interatomic distance. Therefore, ultrathin metal oxide layers can serve as a model system to investigate intraparticle transport which may be useful for a better understanding of the electric transport in a network of interconnected nanoparticles. Metal oxides are wide band gap materials and electronic states in the forbidden gap are crucial for the charge transport. For example, the importance of defects for electronic transport has been shown for porous TiO_2 electrodes⁶ and thin Ta_2O_5 layers.⁴

There are only a few experimental techniques allowing to obtain information about electronic states in ultrathin metal oxides. Photovoltage (PV) measurements have the advantages to be contactless and to give information about the type of states. This makes PV measurements more universal than other techniques such as photoelectron spectroscopy⁷ or internal electron photoemission.⁸ We apply the transient photovoltage⁹ and spectral dependent photovoltage^{10,11} techniques to investigate trap states in ultra thin metal oxide

layers. As known, a photovoltage arises whenever excess charge carriers are separated in space. For example, the separation of negatively and of positively charged sheets with a density of only 10^{10} cm^{-2} by 1 nm would cause a reasonable voltage drop of the order of 100 μV .

In this work we observed photovoltage signals at metal oxide (thickness of the order of nanometers) / metal structures. The photovoltage measurements have been used to characterize trap states in ultrathin metal oxide layers. Several metal oxide layers ($\text{TiO}_2, \text{Cu}_2\text{O}, \text{ZnO}$) with different dominating traps (hole traps, electron and hole traps, electron traps, respectively) are investigated by spectral and transient PV techniques. A model of the relaxation of the photovoltage signal including recombination of spatially separated excess carriers due to tunneling and thermal emission is developed for the case when only one type of charge carriers is predominantly trapped in the metal oxide layer.

II. EXPERIMENTAL DETAILS

Layers of $\text{TiO}_2, \text{Cu}_2\text{O}$, and ZnO were prepared at Ti, Cu, and Zn substrates, respectively. The TiO_2 (anatase) layer was obtained by standard anodic oxidation in the galvanostatic regime in a 0.5 M H_2SO_4 electrolyte and a current of 1 mA/cm^2 was supported until the final voltage U_0 was reached. The thickness d of the anodic layers of 20 nm is determined by $U_0=9.5 \text{ V}$. Copper oxide was prepared by thermal oxidation of Cu at 150 °C for 2 h [growth rate about 5 nm/h (Ref. 12)]. The ZnO layer was formed by prolonged native oxidation at room temperature. The thickness of the Cu_2O and ZnO layers was about 10 nm.

The PV measurements were carried out in the standard parallel plate capacitor arrangement.¹⁰ The capacitor consisted of the metal oxide layer on the metal substrate, a

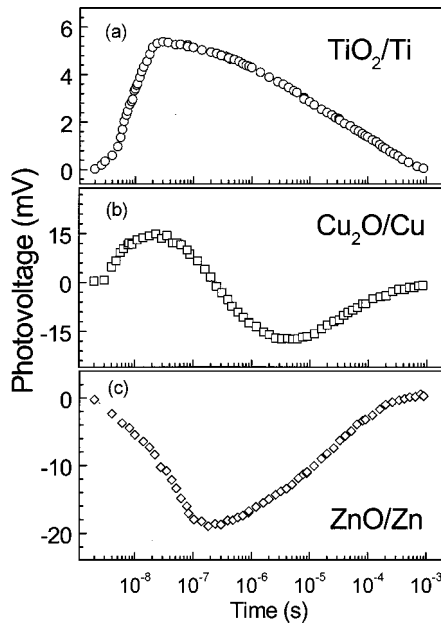


FIG. 1. Photovoltage transients for ultrathin layers of TiO_2 (a), Cu_2O (b), and ZnO (c) at the Ti, Cu, and Zn metal substrates, respectively.

10 μm thick mica spacer and a semitransparent Cr electrode (diameter 5 mm). The metal substrate and the semitransparent Cr electrode served as the reference and probe electrodes, respectively. The PV transients were excited with single pulses of a N_2 laser (photon energy 3.7 eV, duration time of a pulse 5 ns, density per pulse between 10^{-2} and $10^2 \mu\text{J}/\text{cm}^2$) and measured on a time scale from 10 ns to 10 ms. A 1000 W Xe lamp with a quartz-prism monochromator was used to excite the spectral dependent PV in the range of 1–4 eV. The light was chopped with the frequency of 60 Hz. The presented PV spectra are normalized to the photon flux $\Phi(U_{\text{PV}}/\Phi)$ for the regime of weak excitation (PV signal depends linearly on the photon flux).

III. FORMATION OF THE PHOTOVOLTAGE

A. Preferential trapping of electrons or holes

Figure 1 shows typical PV transients for different ultrathin metal oxide layers (TiO_2 , Cu_2O , ZnO) on the respective metal surfaces. The PV transients were excited by light with photon energy above the band gap of the metal oxides [3.42,¹³ 2.0,¹⁴ and 3.3 eV (Ref. 15) for TiO_2 (anatase), Cu_2O and ZnO , respectively]. Depending on the metal oxide, the PV signal can be positive (TiO_2) or negative (ZnO) or also may change the sign in time (Cu_2O). A positive (negative) PV signal means that negative (positive) charge carriers are moving towards the metal surface so that preferentially positive (negative) charge carriers stay trapped in the ultrathin metal oxide layer.

In the usual case, both electron and hole traps are present in metal oxide films, but the concentrations and distributions of them may be very different. No PV signal would appear if both electrons and holes are trapped homogeneously in the metal oxide layer. For example, for the ZnO layer the maxi-

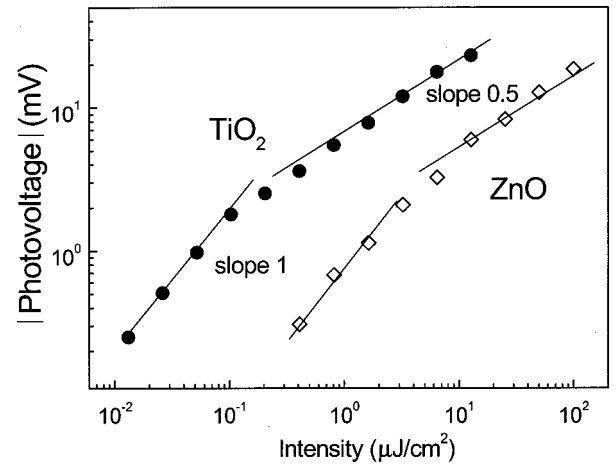


FIG. 2. Dependence of the absolute value of the PV amplitude on the excitation intensity for the TiO_2 and ZnO layers.

imum of the negative PV signal is reached only after about 200 ns (for comparison, the duration time of the laser pulse was 5 ns) which gives an imagination about the release time of trapped holes in this case. In difference, the release time is very short for electrons in the TiO_2 layer. The situation is more complicated in the Cu_2O layer where the concentration of trapped holes is larger than the concentration of trapped electrons at the shorter times but where the release time is much shorter for the holes.

Surface states at the metal oxides are changed immediately with changing the ambient gas atmosphere (air, vacuum, adsorbed water, and oxygen).¹⁰ However, the PV signal did change only very slowly in time after changing the ambience. This demonstrates that the traps being responsible for the formation of the PV signal in ultrathin metal oxide layers are related to the bulk of the metal oxides.

B. Limitation of the photovoltage amplitude

The intensity dependence of the absolute values of the PV amplitude for the TiO_2 and ZnO layers (Fig. 2) is a linear function of the intensity for small excitation level and obeys a square root dependence at higher intensities. A linear dependence of the PV signal on the excess carriers concentration is considered in the small signal case. The square root dependence of the excess carrier concentration, and therefore of the PV, on the excitation intensity is determined by limitation due to bimolecular recombination and has been recently discussed.¹⁶

C. States in the forbidden gap

Figure 3 depicts the spectral dependent PV for the different ultrathin metal oxide layers (TiO_2 , Cu_2O , ZnO) on the respective metal surfaces. The PV signals were normalized to the photon flux. The sign of the spectral dependent PV at 3.7 eV is in agreement with the sign of the transient PV signal for the TiO_2 and ZnO layers. The appearance of the PV at around 3.15 eV for the TiO_2 layer implements the existence of electronic states essentially below the band gap of anatase.

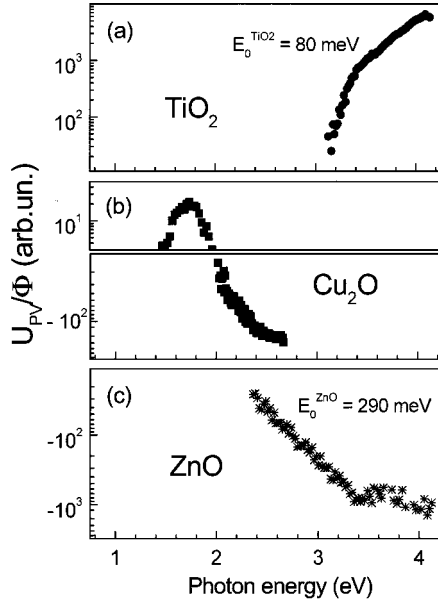


FIG. 3. Photovoltage spectra for the TiO₂ (a), Cu₂O (b), and ZnO layers (c).

The energy of the exponential tail below the band gap is $E_0^{\text{TiO}_2} = 80$ meV for the ultrathin TiO₂ layer what is in very good agreement with measurements on porous TiO₂ layers by spectral photoconductivity^{17,18} or PV.¹⁰ The exponential tails are more extended in the ultrathin ZnO layer ($E_0^{\text{ZnO}} = 290$ meV) than for the TiO₂ layer. As remark, the value of E_0^{ZnO} is usually lower for thick ZnO layers.¹⁵

For the Cu₂O layer, the PV signal is positive for excitation with photon energies below the band gap and negative when the energy of the exciting photons is above the band gap. The positive PV signal below 2 eV can be attributed to the excitation of electrons from occupied states near the valence band edge into the conduction band from where the electrons can easily reach the metal surface.

IV. RELAXATION OF THE PHOTOVOLTAGE

A. Recombination of spatially separated charge carriers

The overlap of the electron and hole wave functions determines the recombination rate of spatially separated charge carriers (spatially dependent recombination). The spatially dependent recombination is well known as one mechanism for persistent photocurrents. Whenever spatially dependent recombination of excess charge carriers takes place (for example, distance-dependent donor-acceptor recombination¹⁹ or recombination between the free electrons and localized centers by means of tunneling²⁰) the decay of the photocurrent signal obeys logarithmic law.²¹ The situation will be more complicated for the decay of the PV transients.

Lets consider that holes are trapped homogeneously in the metal oxide layer and that electrons tunnel from the metal substrate through the oxide to the trapped hole. The rate of the disappearance of holes can be written as²¹

$$\frac{dp(x,t)}{dt} = -\frac{p(x,t)}{\tau} \exp\left(-\frac{2x}{a}\right), \quad (1)$$

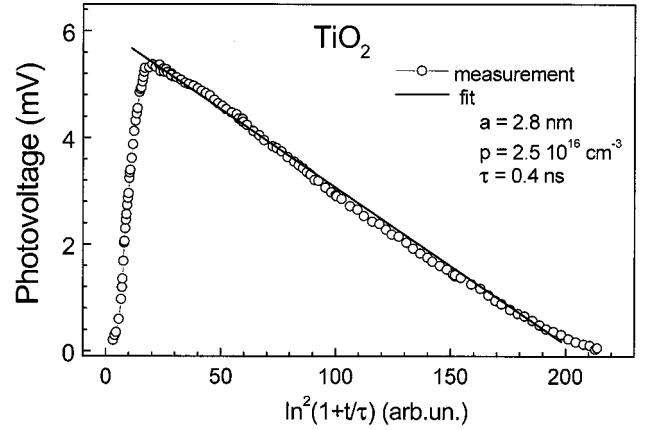


FIG. 4. Measured (open circles) and simulated by Eq. (3) (line) PV transients for the TiO₂ layer. Simulations are made according to the spatially dependent recombination model with parameters $p_0 = 2.5 \times 10^{16} \text{ cm}^{-3}$, $a = 2.8 \text{ nm}$, $\tau = 0.4 \text{ ns}$.

where $x, t, p(x, t), \tau$, and a are the distance from the metal-substrate/metal-oxide interface, time, excess hole concentration, lifetime without spatial separation, and the Bohr radius of trapped holes. The PV signal is determined by the non-compensated positive charge which is given by p_0 at the starting time $t=0$.

The time dependent photovoltage signal can be found if integrating twice the Poisson equation while the hole concentration $p(x, t)$ will be taken from Eq. (1):

$$U(t) = \frac{e}{\epsilon \epsilon_0} \int_0^d dx \int_0^x p(y, t) \exp\left[-\frac{t}{\tau} \exp\left(-\frac{2x}{a}\right)\right] dy, \quad (2)$$

where e is the elementary charge, $\epsilon_0 = 8.85 \times 10^{-12} \text{ F/m}$, ϵ is a dielectric constant of the layer. This expression can be simplified in the case of $t \gg \tau$ (so-called sharp-front approximation²¹)

$$U(t) = \frac{e}{2\epsilon \epsilon_0} p_0 d^2 \left[1 - \left(\frac{a}{2d}\right)^2 \ln^2\left(1 + \frac{t}{\tau}\right) \right]. \quad (3)$$

For ultrathin TiO₂ layers, the PV signal is determined practically only by hole traps and Eq. (3) can be applied to the analysis of the decay of the PV transients. The measured (open circles) and calculated with Eq. (3) (line) PV transients of the TiO₂ layer are plotted in Fig. 4. The transients decay linearly in $\ln^2(1+t/\tau)$ units for $t > \tau$. The value of p_0 can be found from the PV amplitude which is given by $U_{\text{PV}}^{\text{ampl}} = e p_0 d^2 / 2\epsilon \epsilon_0$. From the fit of the measured PV transient one gets the values of the Bohr radius of the trapped hole ($a = 2.8 \text{ nm}$), the initial concentration of the trapped holes ($p_0 = 2.5 \times 10^{16} \text{ cm}^{-3}$ for the case shown in Fig. 4) and the lifetime without spatial separation ($\tau = 0.4 \text{ ns}$). For the relaxation of the PV transients in ZnO or Cu₂O layers, a simple model as in Eq. (3) can not be given.

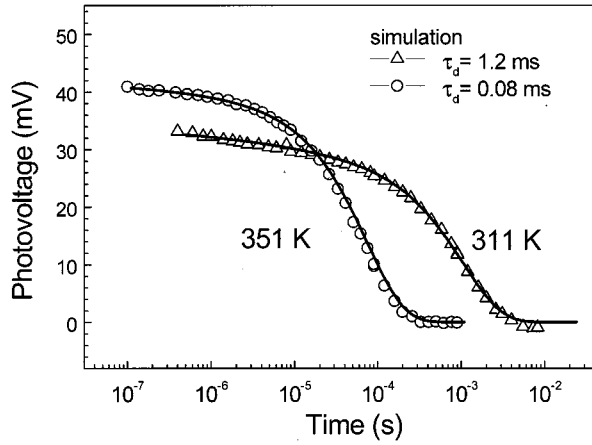


FIG. 5. Measured (symbols) and simulated (lines) PV transients for the TiO_2 layer at two temperatures. Thermal emission of holes (detrapping times of $\tau_d=1.2$ and 0.08 for 311 and 351 K, respectively) is included into the spatially dependent recombination model. The other parameters of the simulated PV transients are $p_0 = 1.5\text{--}2 \times 10^{17} \text{ cm}^{-3}$, $a=2.8 \text{ nm}$, $\tau=0.4 \text{ ns}$.

B. Role of thermal emission at higher temperatures

For increasing temperature, thermal emission becomes important for the relaxation of the separated charge and a thermally activated time constant (detrapping time τ_d) appears. In the case that the relaxation of the excess carrier concentration is determined only by emission and tunneling, p_0 in Eq. (3) has to be replaced by

$$p(t) = p_0 \exp\left(-\frac{t}{\tau_d}\right) \quad (4)$$

with

$$\tau_d = \tau_d^0 \exp\left(\frac{E_A}{kT}\right), \quad (5)$$

where E_A is the activation energy and τ_d^0 is the pre-exponential factor.

Figure 5 shows measured (symbols) and simulated (lines) PV transients for the TiO_2 layer at 311 and 351 K. The PV transients become shorter with increasing temperature (τ_d is 0.08 and 1.2 ms at 351 and 311 K, respectively). The PV amplitude increases with increasing temperature indicating to a partial compensation of trapped holes by trapped electrons at lower temperatures. The trapped electrons escape from the metal oxide layer much faster than the trapped holes with increasing temperature.

The activation energy depends on the intensity of the exciting light pulse. This is demonstrated in Fig. 6. E_A ranges between 0.25 and 0.32 eV. The excitation intensities are related to different values of p_0 which can be obtained from the PV amplitudes. The correlation between p_0 and E_A is given in the inset of Fig. 6 (p_0 is taken for room temperature). One should remark that the exact value of p_0 is not known due to the partial compensation by trapped electrons.

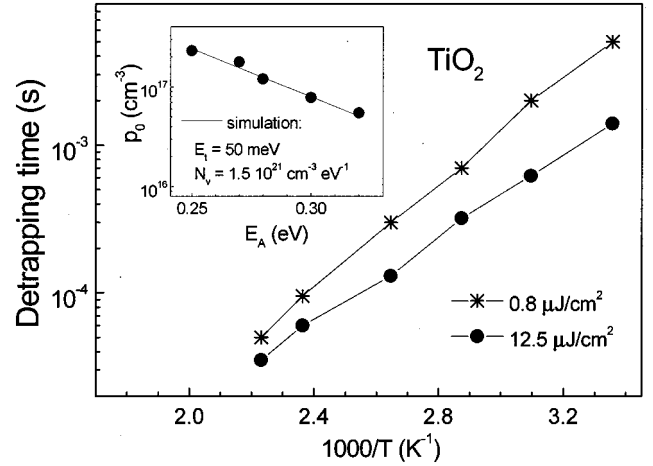


FIG. 6. Arrhenius plot of detrapping times for holes of the TiO_2 layer. The inset shows the correlation between the activation energy of the detrapping time and p_0 .

For the given temperature range, p_0 did increase by up to 40% from room temperature to 450 K.

The decay of the PV transient at higher temperatures is caused by thermal emission of holes trapped in the TiO_2 layer. We point out, that the barrier of 1.3 eV (Ref. 22) between the TiO_2 and the Ti is much higher than E_A and that therefore the emission of electrons from the Ti into the TiO_2 layer can be neglected. In the case of an exponential distribution of trap states (exponential tails at the valence band edge), the correlation between p_0 and E_A can be used to obtain the tail parameter ($E_{t(V)}$) and the density of states at the valence band (N_V). The values of $E_{t(V)}$ and N_V are 0.05 ± 0.01 eV and $10^{21} \text{ eV}^{-1} \text{ cm}^{-3}$, respectively. The value of $E_{t(V)}$ (50 meV) is significantly below $E_0^{\text{TiO}_2}$ (80 meV) which has been obtained from the spectral depen-

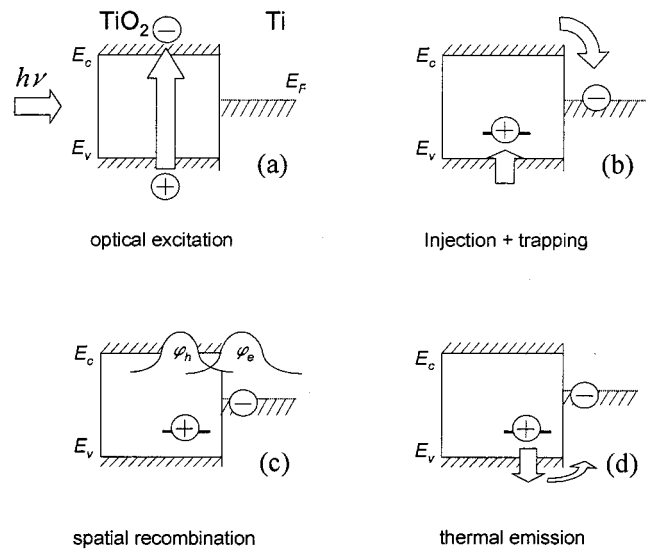


FIG. 7. Overview of the elementary processes of the trap limited PV in case of preferential hole trapping in the metal oxide layer.

dent PV measurements. This difference is not surprising since the spectral dependent PV measurement is sensitive to the combination of the exponential tails at the valence and conduction bands while τ_d is sensitive only to the exponential tail at the valence band.

The pre-exponential parameter in Eq. (5) is given by the effective density of states at the valence band (N_0), the thermal velocity of carriers (v_{th}) and the trapping cross section (σ): $(\tau_d^0)^{-1} = \sigma \times N_0 \times v_{th}$. The experimentally obtained value of $(\tau_d^0)^{-1}$ is $5 \times 10^8 \text{ s}^{-1}$. If taking a thermal velocity of a hole with the free electron mass, one would obtain a capture cross section for holes in ultrathin layers of anodic TiO_2 of the order of $3 \times 10^{-18} \text{ cm}^2$.

V. CONCLUSIONS

Trap limited PV is shown to be a general phenomenon for ultrathin metal oxides. Figure 7 summarizes the elementary processes for the case of preferential hole trapping in the metal oxide. Excess electrons and holes are generated during illumination with photon energy $h\nu$ larger than the band gap

[Fig. 7(a)]. Excess electrons are injected into the metal substrate and excess holes are preferentially trapped [Fig. 7(b)]. This leads to the formation of the PV signal. The amount of trapped charge is limited by bimolecular recombination at high excitation intensities. At lower temperatures, the decay of the PV is determined by the overlap of the wave functions for electrons (φ_e) and holes (φ_h) resulting in the recombination of spatially separated excess carriers due to tunneling [Fig. 7(c)]. At higher temperatures, thermal emission accelerates the relaxation of the PV signal [Fig. 7(d)]. This simple model holds for ultrathin anodic TiO_2 layers with dominating hole traps. With respect to the elementary processes, the trap limited PV can be applied to study electronic states in any ultrathin semiconductor layer at a metal substrate.

ACKNOWLEDGMENTS

V.D. and V.K. are grateful to the Deutsche Forschungsgemeinschaft and the Alexander-von-Humboldt Stiftung, respectively, for financial support.

*Corresponding author, e-mail address:

vduzhko@physik.tu-muenchen.de

¹B. O Regan and M. Graetzel, *Nature (London)* **353**, 737 (1991).

²E. Topoglidis, A. Cass, G. Gilardi, S. Sadeghi, N. Beaumont, and J. Durrant, *Anal. Chem.* **70**, 5111 (1998).

³N. Serpone and R. Khairutdinov, *Application of Nanoparticles in the Photocatalytic Degradation of Water Pollutants* (Elsevier, Amsterdam, 1996), Vol. 103, p. 417.

⁴R. Fleming, D. Lang, C. Jones, M. Steigerwald, D. Murphy, G. Alers, Y. Wong, R. van Dover, J. Kwo, and A. Sergent, *J. Appl. Phys.* **88**, 850 (2000).

⁵R. Breckenridge and W. Hosler, *Phys. Rev.* **91**, 793 (1953).

⁶J. Nelson, S.A. Haque, D.R. Klug, and J.R. Durrant, *Phys. Rev. B* **63**, 205321 (2001).

⁷See, for example, D. Eastman and J. Freeauf, *Phys. Rev. Lett.* **34**, 395 (1975).

⁸V. Afanasev, M. Houssa, A. Stesmans, and M. Heyns, *Appl. Phys. Lett.* **78**, 3073 (2001).

⁹E.O. Johnson, *J. Appl. Phys.* **28**, 1349 (1957).

¹⁰V. Duzhko, V.Yu. Timoshenko, F. Koch, and Th. Dittrich, *Phys. Rev. B* **64**, 075204 (2001).

¹¹See, for example, L. Kronik and Y. Shapira, *Surf. Sci. Rep.* **37**, 1 (1999) and references therein.

¹²R.J. Blattner, C.A. Evans, and A.J. Braundmeier, *J. Vac. Sci. Technol.* **14**, 1132 (1977).

¹³H. Tang, F. Levy, H. Berger, and P.E. Schmid, *Phys. Rev. B* **52**, 7771 (1995).

¹⁴A. Rakhshani, *J. Appl. Phys.* **69**, 2365 (1991).

¹⁵V. Srikant, D. Clarke, *J. Appl. Phys.* **81**, 6357 (1997); V. Srikant, D. Clarke, *ibid.* **83**, 5447 (1998).

¹⁶V. Kytin, V. Duzhko, J. Rappich, and Th. Dittrich, *Phys. Status Solidi A* **185**, R1 (2001).

¹⁷See for example, Th. Dittrich, *Phys. Status Solidi A* **182**, 447 (2000), and references therein.

¹⁸R. Könenkamp, *Phys. Rev. B* **61**, 11 057 (2000).

¹⁹D.G. Thomas, J.J. Hopfield, and W.M. Augustyniak, *Phys. Rev.* **140**, 202 (1965).

²⁰E.F. Schubert, A. Fischer, and K. Ploog, *Phys. Rev. B* **31**, 7937 (1985).

²¹H.J. Queisser and D.E. Theodorou, *Phys. Rev. B* **33**, 4027 (1986).

²²D.M. Hanson, R. Stockbauer, and T.E. Madey, *Phys. Rev. B* **24**, 5513 (1981).